

# Solid-State and High-Resolution Liquid $^{119}\text{Sn}$ NMR Spectroscopy of Some Monomeric, Two-Coordinate Low-Valent Tin Compounds: Very Large Chemical Shift Anisotropies

Barrett E. Eichler, Brian L. Phillips, Philip P. Power,\* and Matthew P. Augustine\*

Departments of Chemistry and Materials Science, One Shields Avenue, University of California, Davis, California 95616

Received May 12, 2000

High-resolution liquid- and solid-state  $^{119}\text{Sn}$  NMR spectroscopy was used to study the bonding environment in the series of monomeric, two-coordinate Sn(II) compounds of formula  $\text{Sn}(\text{X})\text{C}_6\text{H}_3\text{-2,6-Trip}_2$  ( $\text{X} = \text{Cl}$ ,  $\text{Cr}(\eta^5\text{-C}_5\text{H}_5)(\text{CO})_3$ , t-Bu,  $\text{Sn}(\text{Me})_2\text{C}_6\text{H}_3\text{-2,6-Trip}_2$ ; Trip =  $\text{C}_6\text{H}_2\text{-2,4,6-i-Pr}_3$ ). The trends in the principal components of the chemical shift tensor extracted from the solid-state NMR data were consistent with the structures determined by X-ray crystallography. Furthermore, the spectra for the first three compounds displayed the largest  $^{119}\text{Sn}$  NMR chemical shift anisotropies (up to 3798 ppm) of any tin compound for which data are currently available. Relaxation time based calculations for the dimetallic compound  $2,6\text{-Trip}_2\text{H}_3\text{C}_6\text{Sn-Sn}(\text{Me})_2\text{C}_6\text{H}_3\text{-2,6-Trip}_2$  suggests that the chemical shift anisotropy for the two-coordinate tin center may be as much as ca. 7098 ppm, which is as broad as the 1 MHz bandwidth of the NMR spectrometer.

## Introduction

The use of  $^{119}\text{Sn}$  NMR spectroscopy has proven to be an invaluable structural probe in all areas of tin chemistry.<sup>1</sup> A large body of data is now available<sup>2</sup> which demonstrates that  $^{119}\text{Sn}$  NMR studies provide accurate, relatively easily obtainable information on the bonding to the tin atom. In many cases the most important spectroscopic parameter available from these studies is the value of the chemical shift ( $\delta$ ). While much of the chemical shift data concern isotropic  $^{119}\text{Sn}$  shift values measured in solution, solid-state  $^{119}\text{Sn}$  NMR measurements usually afford more detailed information involving the  $\delta_{11}$ ,  $\delta_{22}$ , and  $\delta_{33}$  components of the nuclear shielding tensor, information that can provide considerably more insight into the bonding at tin.<sup>3</sup> Monomeric, two-coordinate tin(II) compounds (e.g.,  $\text{SnR}_2$ ; R = alkyl,<sup>4</sup> aryl,<sup>5</sup> amide,<sup>6</sup> or alkoxide<sup>7</sup> groups) whose bonding is often more complex than that in tin(IV) compounds owing to the presence of a formally empty, nonbonding p-orbital and a stereochemically active lone pair (in an orbital that is mostly 5s in character) at the tin centers, are particularly amenable to solid-state  $^{119}\text{Sn}$  NMR investigation. Unfortunately, there are no such studies available for this important compound class. This may be due to the fact that monomeric compounds of this kind are not numerous and that they usually require careful handling owing to their extreme air and moisture sensitivity. Nonetheless, studies<sup>8</sup> on the related compounds such as  $\text{R}_2\text{-}$

$\text{SnSnR}_2$  (R =  $\text{CH}(\text{SiMe}_3)_2$ ), which consist of weakly dimerized  $\text{SnR}_2$  units, clearly demonstrate large chemical shift anisotropy, as evidenced by the principal values  $\delta_{11} = 1600$ ,  $\delta_{22} = 400$ , and  $\delta_{33} = 100 \pm 20$  ppm, which is an order of magnitude greater than that seen in Sn(IV) species. These values suggest strong deshielding along the axis in the  $\text{SnC}_2$  ligand plane and perpendicular to the Sn–Sn bond (i.e.,  $\delta_{11}$ ) and much greater shielding along the axis perpendicular to the  $\text{SnC}_2$  coordination plane at tin (i.e.,  $\delta_{33}$ ). We were therefore anxious to record the solid-state spectra of some monomeric two-coordinate Sn(II) species with the expectation that such a study would reveal large anisotropies in their chemical shift tensors which would help elucidate the nature of the bonding in these complexes. The results of these studies are now described.

## Experimental Section

The synthesis of  $\text{Sn}(\text{Cl})\text{C}_6\text{H}_3\text{-2,6-Trip}_2$ <sup>9</sup> and  $\{\text{Sn}(\text{Cl})\text{C}_6\text{H}_3\text{-2,6-Mes}_2\}_2$ <sup>10</sup> (Mes =  $\text{C}_6\text{H}_2\text{-2,4,6-(CH}_3)_3$ ) have been previously reported. The compounds  $\text{Sn}(\text{X})\text{C}_6\text{H}_3\text{-2,6-Trip}_2$  ( $\text{X} = \text{Cr}(\eta^5\text{-C}_5\text{H}_5)(\text{CO})_3$ , t-Bu, or  $\text{Sn}(\text{Me})_2\text{C}_6\text{H}_3\text{-2,6-Trip}_2$ ) were synthesized by the reaction of  $\text{Sn}(\text{Cl})\text{C}_6\text{H}_3\text{-2,6-Trip}_2$  with  $\text{Na}[\text{Cr}(\eta^5\text{-C}_5\text{H}_5)(\text{CO})_3]$ , t-BuLi, or MeLi, respectively. Full details of the synthesis, structural characterization, and reactions of these three compounds will be provided separately.<sup>11</sup> Solid-state  $^{119}\text{Sn}$  NMR spectra were recorded under conditions of magic angle spinning at 9.4 T using a Chemagnetics Infinity NMR spectrometer and probehead configured for 7.5 mm (o.d.) rotors. A combination of fast relaxation and restricted sample quantities typically limited data accumulation to between one and four rotational echoes. The absolute value of the Fourier transform of the first rotational echo provided pure phase powder patterns that were used to determine  $\delta_{\text{nn}}$  values.<sup>12</sup> Isotropic liquid shifts were obtained using both this Chemagnetics solid-state

- (1) Kennedy, J. D.; McFarlane, W. In *Multinuclear NMR*; Mason, J., Ed.; Plenum: New York, 1987; Chapter 4.
- (2) Wrackmeyer, B. *Annu. Rep. NMR Spectrosc.* **1999**, *38*, 203.
- (3) Duncan, T. M. *A Compilation of Chemical Shift Anisotropies*; Farragut Press: Chicago, 1990.
- (4) Davidson, P. J.; Lappert, M. F. *J. Chem. Soc. Chem. Commun.* **1973**, 317.
- (5) Weidenbruch, M.; Schaeffel, J.; Schäfer, A.; Peters, K.; von Schnering, H. G.; Marsmann, H. *Angew. Chem., Int. Ed. Engl.* **1994**, *33*, 1846.
- (6) Harris, D. H.; Lappert, M. F. *J. Chem. Soc. Chem. Commun.* **1974**, 895.
- (7) Cetinkaya, B.; Gümrükcü, I.; Lappert, M. F.; Atwood, J. L.; Rogers, R. D.; Zaworotko, M. *J. Am. Chem. Soc.* **1980**, *102*, 2088.
- (8) Zilm, K.; Lawless, G. A.; Merrill, R. M.; Millar, J. M.; Webb, G. G. *J. Am. Chem. Soc.* **1987**, *109*, 7236.

- (9) Pu, L.; Senge, M. O.; Olmstead, M. M.; Power, P. P. *J. Am. Chem. Soc.* **1998**, *120*, 12682.
- (10) Simons, R. S.; Pu, L.; Olmstead, M. M.; Power, P. P. *Organometallics* **1997**, *16*, 1920.
- (11) (a) Eichler, B. E.; Power, P. P. *Inorg. Chem.* **2000**, *39*, 5444. (b) Eichler, B. E.; Power, P. P. Unpublished work.
- (12) Chingas, G.; Frydman, L.; Barrall, G.; Hartwood, J. S. in *NMR Spectroscopy: History, Theory and Applications*; Blumlich, B.; Kuhn, W., Eds.; VCH: Weinheim, 1992; pp 373–393.

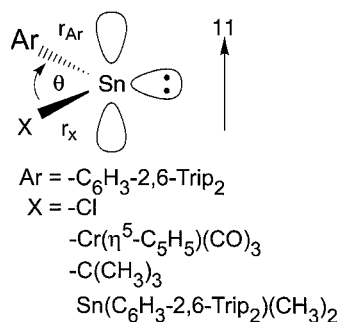


**Figure 1.** Model of the Sn(II) metal center structure in the compounds used in this study. The bond lengths  $r_{\text{Ar}}$  between Sn and Ar = 2,6-Trip<sub>2</sub>C<sub>6</sub>H<sub>3</sub> and  $r_{\text{x}}$  between Sn and X = Cl, Cr( $\eta^5$ -C<sub>5</sub>H<sub>5</sub>)(CO)<sub>3</sub>, t-Bu, and Sn(Me)<sub>2</sub>(C<sub>6</sub>H<sub>3</sub>-2,6-Trip<sub>2</sub>) and Ar–Sn–X bond angle  $\theta$  determined by X-ray crystallography are summarized in Table 2.

**Table 1.** Summary of  $^{119}\text{Sn}$  Liquid State Chemical Shifts of 2,6-Trip<sub>2</sub>H<sub>3</sub>C<sub>6</sub>SnX (Trip = C<sub>6</sub>H<sub>2</sub>-2,4,6-i-Pr<sub>3</sub>, X = Cl, Cr( $\eta^5$ -C<sub>5</sub>H<sub>5</sub>)(CO)<sub>3</sub>, t-Bu, Sn(Me)<sub>2</sub>C<sub>6</sub>H<sub>3</sub>-2,6-Trip<sub>2</sub>)

X	$\delta_{\text{liq}}$ (ppm)	reference
Cl	793.4	10
Cr( $\eta^5$ -C <sub>5</sub> H <sub>5</sub> )(CO) <sub>3</sub>	2,297.9	11b
t-Bu	1,904.4	11a
Sn(Me) <sub>2</sub> C <sub>6</sub> H <sub>3</sub> -2,6-Trip <sub>2</sub> <sup>a</sup>	2856.9	11a
	257.4 <sup>a</sup>	
{Sn( $\mu$ -Cl)C <sub>6</sub> H <sub>3</sub> -2,6-Mes <sub>2</sub> )} <sub>2</sub>	625.2	9

<sup>a</sup> Chemical shift of the tetravalent tin atom.

system and a Varian Inova NMR spectrometer operating at 9.4 T. Solid-state isotropic chemical shifts for samples giving several rotational echoes were obtained from the magic angle spinning centerband.

## Results and Discussion

To better understand bonding and electronic structure in the series of compounds of formula Sn(X)C<sub>6</sub>H<sub>3</sub>-2,6-Trip<sub>2</sub> illustrated schematically in Figure 1 where X = Cl, t-Bu, Cr( $\eta^5$ -C<sub>5</sub>H<sub>5</sub>)(CO)<sub>3</sub>, and Sn(Me)<sub>2</sub>(C<sub>6</sub>H<sub>3</sub>-2,6-Trip<sub>2</sub>),  $^{119}\text{Sn}$  NMR data in both the liquid phase and the solid state were recorded. It is well-known that the isotropic liquid state  $^{119}\text{Sn}$  chemical shift  $\delta_{\text{liq}}$  is sensitive to both valence and electronic structure.<sup>1,2</sup> For example, Sn(IV) compounds tend to be more shielded and resonate further upfield ( $-1100 \text{ ppm} < \delta_{\text{liq}} < +200 \text{ ppm}$ ) than deshielded Sn(II) compounds ( $+200 \text{ ppm} < \delta_{\text{liq}} < +5000 \text{ ppm}$ ).<sup>2</sup> A summary of  $\delta_{\text{liq}}$  in ppm for the compounds in Figure 1 is shown in Table 1, along with additional data for the related dinuclear tin complex {Sn( $\mu$ -Cl)C<sub>6</sub>H<sub>3</sub>-2,6-Mes<sub>2</sub>)}<sub>2</sub>,<sup>10</sup> which is associated through chloride bridging. The shifts for all of the compounds shown in Figure 1 are greater than 200 ppm which indicates that the tin is in the oxidation state +2 (note that the formal oxidation states of the tin atoms in 2,6-Trip<sub>2</sub>H<sub>3</sub>C<sub>6</sub>Sn–Sn(Me)<sub>2</sub>C<sub>6</sub>H<sub>3</sub>-2,6-Trip<sub>2</sub> are Sn(I) and Sn(III) although they are divalent and tetravalent). However, there seems to be no apparent trend in the chemical shifts of the series with X = Cl, Cr( $\eta^5$ -C<sub>5</sub>H<sub>5</sub>)(CO)<sub>3</sub>, t-Bu, and Sn(Me)<sub>2</sub>(C<sub>6</sub>H<sub>3</sub>-2,6-Trip<sub>2</sub>). For example, the electronegativity of the atoms bound to tin increases in the order: Cr(1.6), Sn(1.96), C(2.55), Cl(3.16), suggesting that electron density at the tin nucleus should be depleted in the same order and thereby generate a chemical shift trend opposite to what is observed. Other explanations for the order of  $\delta_{\text{liq}}$  for these compounds based on ligand electron withdrawing and donating characteristics as well as their  $\pi$ -back-bonding capacity also lead to predictions inconsistent with the observed  $\delta_{\text{liq}}$  trend. One plausible explanation is that the paramagnetic shielding, a reflection of the mixing of ground and excited states, is increased rather than decreased by more electronegative substituents.<sup>13</sup>

Since the HOMO–LUMO gap in group 14 carbene analogues increases with more electronegative substituents, a smaller contribution to the paramagnetic shielding is expected to produce a more upfield resonance (since paramagnetic effects augment the applied field). This consideration has been used to account for the higher field shifts for tin(II) amides and alkoxides.<sup>2,14,15</sup> However, the observed isotropic chemical shift is not only a sum of paramagnetic and diamagnetic terms, but also a function of directionally dependent components.

In the absence of unusual averaging effects, the liquid-state shift is equal to the isotropic chemical shift, the average  $\delta_{\text{iso}} = (\delta_{11} + \delta_{22} + \delta_{33})/3$  of the three principal components  $\delta_{11}$ ,  $\delta_{22}$ , and  $\delta_{33}$  of the chemical shift tensor. Here  $\delta_{11}$  and  $\delta_{33}$  label the downfield and upfield edges of the observed NMR spectrum in the solid state whereas  $\delta_{22}$  represents the frequency that corresponds to a singularity in the powder pattern where the spectral amplitude tends to infinity. Physically, these  $\delta_{\text{nn}}$  values describe the shape of an ellipsoid in three dimensions in the principal axis system of the chemical shift tensor. This shape is related to the topology of the electronic wave function at the site of the nucleus and can therefore lead to details about chemical bonding. The size of and difference between  $\delta_{\text{nn}}$  values for a particular site is a strong function of the symmetry and structure of the bonding environment. This structural dependence is illustrated by a comparison of shift tensor values for tetraphenyl tin, SnPh<sub>4</sub>,<sup>16</sup> and the already mentioned<sup>8</sup> R<sub>2</sub>SnSnR<sub>2</sub> (R = CH(SiMe<sub>3</sub>)<sub>2</sub>) dimer (which is dissociated to SnR<sub>2</sub> monomers in dilute solution) which have the values  $\delta_{\text{iso}} = -117 \text{ ppm}$  and  $+700 \text{ ppm}$ , respectively. The relaxed tetrahedral environment at tin in SnPh<sub>4</sub> yields an axially symmetric powder pattern with  $\delta_{11} = -90 \text{ ppm}$  and  $\delta_{22} = \delta_{33} = -130 \text{ ppm}$  whereas the less symmetric environment in R<sub>2</sub>SnSnR<sub>2</sub> generates  $\delta_{11} = +1600 \text{ ppm}$ ,  $\delta_{22} = +400 \text{ ppm}$ , and  $\delta_{33} = +100 \text{ ppm}$ , thereby affording an asymmetric powder pattern with record anisotropy  $\chi = 3(\delta_{11} - \delta_{\text{iso}})/2 = 1350 \text{ ppm}$ .

**Chemical Shift Trends in the Sn(X)C<sub>6</sub>H<sub>3</sub>-2,6-Trip<sub>2</sub> Compounds (X = Cl, Cr( $\eta^5$ -C<sub>5</sub>H<sub>5</sub>)(CO)<sub>3</sub>, and t-Bu) and Related Species.** The  $^{119}\text{Sn}$  solid-state NMR spectra shown in Figure 2a–c correspond to the mononuclear compounds in Figure 1 with X = Cl, Cr( $\eta^5$ -C<sub>5</sub>H<sub>5</sub>)(CO)<sub>3</sub>, and t-Bu, respectively. The solid lines represent the actual experimental data while the dashed lines represent fits used to extract  $\delta_{\text{nn}}$  values. The  $\delta_{\text{nn}}$  values for these spectra and the spectra (not shown) for 2,6-Trip<sub>2</sub>H<sub>3</sub>C<sub>6</sub>Sn–Sn(Me)<sub>2</sub>C<sub>6</sub>H<sub>3</sub>-2,6-Trip<sub>2</sub> and {Sn( $\mu$ -Cl)C<sub>6</sub>H<sub>3</sub>-2,6-Mes<sub>2</sub>)}<sub>2</sub> are included in Table 2 along with a calculation of the isotropic chemical shift and the Ar–Sn–X bond angle  $\theta$ , C<sub>Ar–Sn</sub> bond length  $r_{\text{Ar}}$ , and Sn–X bond length  $r_{\text{x}}$  values obtained from X-ray data. It is important to note that the anisotropic chemical shift tensor values for the X = Sn(Me)<sub>2</sub>C<sub>6</sub>H<sub>3</sub>-2,6-Trip<sub>2</sub> compound represent only the Sn(III) site with  $\delta_{\text{liq}} = 257.4 \text{ ppm}$  in Table 1. All attempts at obtaining solid-state data for the Sn(I) site failed, presumably, as discussed later, because the anisotropy  $\chi$  is too large to measure by pulse-Fourier transform techniques at this field strength.

Although the trend in  $\delta_{\text{liq}}$  values in Table 1 for the compounds in the series X = Cl, Cr( $\eta^5$ -C<sub>5</sub>H<sub>5</sub>)(CO)<sub>3</sub>, and t-Bu is not obvious, the variation of each of the  $\delta_{\text{nn}}$  components of the chemical

- Albright, T. A.; Burdett, J. K.; Whangbo, M. H. *Orbital Interactions in Chemistry*; Wiley: New York, 1985; p 127.
- Braunschweig, H.; Chorley, R. W.; Hitchcock, P. B.; Lappert, M. F. *J. Chem. Soc., Chem. Commun.* **1992**, 1311.
- Wrackmeyer, B. *Unkonventionelle Wechselwirkungen in der Chemie metallischer Elemente*; Krebs, B., Ed.; VCH: Weinheim, 1992; pp 111–124.
- Komoroski, R. A.; Parker, R. G.; Mazany, A. M. *J. Magn. Res.* **1987**, 73, 389.

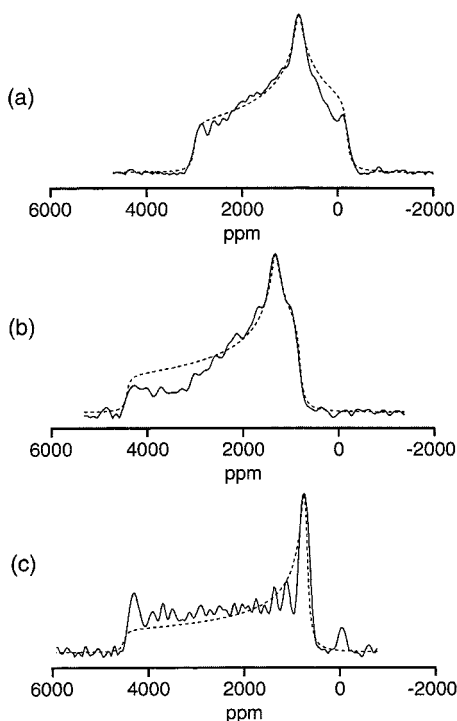


**Figure 2.** Examples of solid-state  $^{119}\text{Sn}$  NMR powder patterns observed in this study. The solid lines represent experimental data for the  $\text{X} = \text{Cl}$ ,  $\text{Cr}(\eta^5\text{-C}_5\text{H}_5)(\text{CO})_3$ , and  $t\text{-Bu}$  compounds in a, b, and c, respectively. The dashed lines indicate the fits used to extract the  $\delta_{11}$ ,  $\delta_{22}$ , and  $\delta_{33}$  shift tensor components.

shift tensor for these compounds can be directly related to structure. Consider both the downfield  $\delta_{11}$  and upfield  $\delta_{33}$  components of the shift tensor. These matrix elements correspond to the minimum and maximum values of the chemical shielding or the minimum and maximum electron density along orthogonal directions in the principal axis system of the chemical shift tensor. With regard to the structure shown in Figure 1, which has both an empty p-orbital and lone electron pair, it is most likely that the 11 direction lies along the symmetry axis of the empty p-orbital whereas the 33 direction involves the hybrid orbital containing the lone electron pair. To be absolutely certain of the orientation of the principal axis system of the shift tensor in the molecular frame, either single crystal measurements or investigation of the relationship between a known dipolar coupling and the principal axis system of the shift tensor would be required. However, in the absence of such measurements this assignment of the 11 and 33 directions appears to be consistent with back-bonding trends and X-ray structural data. The structure in Figure 1 indicates essentially zero electron density along the 11 direction. Therefore, one would expect  $\delta_{11}$  for these compounds to tend toward the bare nucleus value. The finite but large value for  $\delta_{11}$ , coupled with its variation in the order smallest to largest in the sequence  $\text{X} = \text{Cl}$ ,  $< \text{Cr}(\eta^5\text{-C}_5\text{H}_5)(\text{CO})_3$ ,  $< t\text{-Bu}$  can be explained by back-bonding. The filled nonbonding orbitals in the Cl ligand more efficiently overlap the p-orbital on tin than either the d-orbitals on the chromium in the  $\text{Cr}(\eta^5\text{-C}_5\text{H}_5)(\text{CO})_3$  moiety or any projection of C–C  $\sigma$  bond electron density from the  $t\text{-Bu}$  ligand. Of these three X ligands, Cl back-donates the most electron density to the tin, thus shielding the  $^{119}\text{Sn}$  nucleus and causing the  $\delta_{11}$  value to appear farther upfield. The same argument holds for the  $\text{Cr}(\eta^5\text{-C}_5\text{H}_5)(\text{CO})_3$  ligand in comparison to the  $t\text{-Bu}$  ligand since back-bonding orbital overlap is likely to be greater for the former moiety.<sup>2,14,15</sup> The trend in  $\delta_{33}$  values in order

from largest to smallest as  $\text{X} = \text{Cr}(\eta^5\text{-C}_5\text{H}_5)(\text{CO})_3$ ,  $> t\text{-Bu}$ ,  $> \text{Cl}$ , can be rationalized in terms of the variation of the Ar–Sn–X bond angle  $\theta$ . As  $\theta$  decreases from 110.13° to 99.68° in Table 2, the hybrid orbital containing the lone pair gains more s character. This gain in s character at tin translates into increased shielding owing to the increased electron density at the  $^{119}\text{Sn}$  nucleus. Thus the most shielded  $\delta_{33}$  value of  $-165.1$  ppm is observed for the most electronegative substituent  $\text{X} = \text{Cl}$  since this compound has the narrowest interligand angle at tin. The narrowing of the angle is apparently caused by the tendency of the more electronegative ligands to attract the most p-character into the orbitals from the central element to which they are bound, thereby allowing the s-character of the lone pair to increase. Finally, the trend in  $\delta_{22}$  values can be explained from the X-ray data and the structure in Figure 1. Since the direction of the  $\delta_{nn}$  components must be orthogonal to each other,  $\delta_{22}$  must lie in the Ar–Sn–X plane and at an angle of 90° with respect to both  $\delta_{11}$  and  $\delta_{33}$ . In other words, the  $\delta_{22}$  component lies in the coordination plane of tin at a right angle to the  $\delta_{33}$  component that is directed through the lone pair. From Table 2 it can be seen that both  $\delta_{22}$  and  $r_x$  decrease in the order  $\text{X} = \text{Cr}(\eta^5\text{-C}_5\text{H}_5)(\text{CO})_3$ ,  $> \text{Cl}$ ,  $> t\text{-Bu}$  which supports the suggestion that the direction of  $\delta_{22}$  was at an angle of 90° to the 33 direction and close to the Sn–X bond direction in Figure 1. The correlation of  $\delta_{22}$  with bond length is possibly easier to rationalize than the trends for  $\delta_{11}$  and  $\delta_{33}$ . Here the increased bond length indicates that electron density will be depleted from around the metal center thus deshielding the  $^{119}\text{Sn}$  nucleus and causing the  $\text{X} = \text{Cr}(\eta^5\text{-C}_5\text{H}_5)(\text{CO})_3$  compound to resonate farther downfield than the  $\text{X} = t\text{-Bu}$  and Cl compounds. It is important to note that differing energy gaps corresponding to directionally dependent HOMO and LUMO's as obtained from ab initio calculations, such as those performed on a family of singlet carbene molecules where similar trends are observed,<sup>17</sup> would provide further insight into the observed trends in the  $\delta_{nn}$  components by carefully tracking both the paramagnetic and diamagnetic contributions to  $\delta_{nn}$ .

#### Comparison of Liquid- and Solid-State Isotropic Shifts.

It is interesting to compare  $\delta_{\text{liq}}$  for each compound in Table 1 with  $\delta_{\text{iso}}$  in Table 2 calculated from the  $\delta_{nn}$  values and the magic angle centerband isotropic shift  $\delta_{\text{mas}}$  in Table 2. The difference between  $\delta_{\text{iso}}$  and  $\delta_{\text{mas}}$  gives an estimate for the uncertainty of the powder pattern fitting routine due to linebroadening and noise in the spectral data. It is obvious from comparison that  $\delta_{\text{liq}}$  is not equal to  $\delta_{\text{iso}}$ . Closer inspection of the data reveals that there is a ca. 5% difference between  $\delta_{\text{liq}}$  and  $\delta_{\text{iso}}$  values for both the  $\text{X} = \text{Cr}(\eta^5\text{-C}_5\text{H}_5)(\text{CO})_3$  and  $t\text{-Bu}$  compounds. In terms of the data sets shown in Figure 2, this 5% difference translates into a change in  $\delta_{nn}$  values of less than four points. More bothersome, however, are the 17% and 35% difference between  $\delta_{\text{liq}}$  and  $\delta_{\text{iso}}$  for the Sn(II) sites in the  $\{\text{Sn}(\mu\text{-Cl})\text{C}_6\text{H}_3\text{-2,6-Mes}_2\}_2$  and  $\text{X} = \text{Cl}$  compounds respectively and the 19% difference for the Sn(III) site in the  $\text{X} = \text{Sn}(\text{Me})_2(\text{C}_6\text{H}_3\text{-2,6-Trip}_2)$  compound. Barring incomplete averaging effects, chemical exchange, or unusual solvent effects,  $\delta_{\text{liq}}$  should always equal  $\delta_{\text{iso}}$ . The 17% and 19% difference recognized in the dinuclear tin compounds could be due to any or all of these possibilities. These two dinuclear complexes also have two bulky aromatic ligands and are nearly twice the size of the other compounds, thus forcing the tumbling rate in solution to be slower. The decreased tumbling rate in the liquid could lead to incomplete averaging of the shift tensor components and yield a skewed

(17) Wiberg, K. B.; Hammer, J. D.; Keith, T. A.; Zilm, K. W. *J. Phys. Chem. A* **1999**, *103*, 21.

**Table 2.** Summary of  $^{119}\text{Sn}$  Solid-State NMR Data and X-ray Parameters in  $\text{ArSnX}$  Compounds (Ar =  $\text{C}_6\text{H}_3\text{-2,6-Trip}_2$ ; X = Cl,  $\text{Cr}(\eta^5\text{-C}_5\text{H}_5)(\text{CO})_3$ , t-Bu,  $\text{Sn}(\text{Me})_2\text{C}_6\text{H}_3\text{-2,6-Trip}_2$ )

X	$\delta_{11}$ (ppm)	$\delta_{22}$ (ppm)	$\delta_{33}$ (ppm)	$\delta_{\text{iso}}$ (ppm)	$\delta_{\text{mas}}$ (ppm)	$\chi$	$\theta$ (deg)	$r_{\text{x}}$ (Å)	$r_{\text{Ar}}$ (Å)
Cl	3021	826	-165	1227	1176	2691	99.68	2.409	2.180
$\text{Cr}(\eta^5\text{-C}_5\text{H}_5)(\text{CO})_3$	4426	1322	814	2187	—	3358	110.13	2.847	2.214
t-Bu	4494	697	697	1962	1829	3798	101.79	2.228	2.211
$\text{Sn}(\text{Me})_2\text{C}_6\text{H}_3\text{-2,6-Trip}_2^a$	781	111	58	317	263	—	119.3	2.891	2.201
$\{\text{Sn}(\mu\text{-Cl})\text{C}_6\text{H}_3\text{-2,6-Mes}_2\}_2$	1643	866	-259	750	—	—	—	—	- <sup>†</sup>

<sup>a</sup> Chemical shift tensor information for only the Sn(III) site.

value for  $\delta_{\text{liq}}$ . The other possibility for this discrepancy, applicable also to the  $\text{Sn}(\text{Cl})\text{C}_6\text{H}_3\text{-2,6-Trip}_2$  compound, is chemical exchange. As noted<sup>8</sup> by Zilm and co-workers, the  $^{119}\text{Sn}$  NMR spectrum of  $\text{R}_2\text{SnSnR}_2$  (R =  $\text{CH}(\text{SiMe}_3)_2$ ) in liquid phase displays effects of chemical exchange (between the dimer  $\text{R}_2\text{-SnSnR}_2$  and the monomer  $\text{SnR}_2$ ), and the true isotropic shift can only be obtained from solid-state spectra. Examination of the X-ray crystal structures of the two dinuclear tin complexes studied here,  $2,6\text{-Trip}_2\text{H}_3\text{C}_6\ddot{\text{S}}\text{n-Sn}(\text{Me})_2\text{C}_6\text{H}_3\text{-2,6-Trip}_2$  and  $\{\text{Sn}(\mu\text{-Cl})\text{C}_6\text{H}_3\text{-2,6-Mes}_2\}_2$ , and the monomeric X = Cl compound, suggests that only in the case of  $\{\text{Sn}(\mu\text{-Cl})\text{C}_6\text{H}_3\text{-2,6-Mes}_2\}_2$ , where a monomer-dimer equilibrium is possible, could such a process account for the discrepancy between the solid- and liquid-phase spectra.

**Exploration of  $2,6\text{-Trip}_2\text{H}_3\text{C}_6\ddot{\text{S}}\text{n-Sn}(\text{Me})_2\text{C}_6\text{H}_3\text{-2,6-Trip}_2$ .** To further investigate the source of this solid/liquid chemical shift discrepancy and to determine why  $^{119}\text{Sn}$  solid-state NMR spectra for the divalent tin (formally Sn(I)) site in the  $2,6\text{-Trip}_2\text{H}_3\text{C}_6\ddot{\text{S}}\text{n-Sn}(\text{Me})_2\text{C}_6\text{H}_3\text{-2,6-Trip}_2$  compound could not be obtained, its solution  $^{119}\text{Sn}$  NMR spectra were studied in the temperature range  $-80$  °C to  $+25$  °C. At room temperature the  $^{119}\text{Sn}$  solution NMR spectrum contains two peaks at  $+2856.9$  ppm and  $+257.4$  ppm, each flanked by satellites due to a  $^{119}\text{Sn}$ - $^{119}\text{Sn}$   $J$  coupling value of 8332 Hz. It is likely that the  $^{119}\text{Sn}$ - $^{117}\text{Sn}$   $J$  coupling is also present, but this splitting is probably within the broad line width of the satellites. No evidence of peak separation ear-marking different products and no evidence of new peaks were observed in this temperature range. The  $J$  coupling also remained constant with temperature. The chemical shifts  $\delta_{\text{liq}}$  and line width did change with temperature. The shift  $\delta_{\text{liq}}$  for the Sn(I) site shifted upfield while  $\delta_{\text{liq}}$  for the tetravalent (formally Sn(III)) site shifted downfield as the temperature was decreased. Lowering the temperature also increased the line width of the spectrum for each site reflecting the longer rotational correlation time and shorter transverse relaxation time  $T_2$  at lower temperature. This variable temperature data (together with bonding considerations) suggest that chemical exchange between different chemical compounds is unlikely to be the source of the discrepancy between  $\delta_{\text{liq}}$  and  $\delta_{\text{iso}}$  values. The change in  $\delta_{\text{liq}}$  with temperature suggests that it is more likely the large size of the molecules, coupled with the extremely large shift anisotropies shown in Table 2, are the source of this difference. Larger molecules translate into longer correlation times and thus less-efficient motional averaging. For shift anisotropies on the order of tens of ppm, it is likely that decreased motion will not substantially change  $\delta_{\text{iso}}$  from  $\delta_{\text{liq}}$ . On the other hand, where anisotropies on the order of thousands of ppm are observed in the solid state, as they are here, decreased motion could profoundly affect the difference between  $\delta_{\text{liq}}$  and  $\delta_{\text{iso}}$ .

Finally, it is important to comment on the absence of solid-state data in Table 2 for the Sn(I) site in the  $2,6\text{-Trip}_2\text{H}_3\text{C}_6\ddot{\text{S}}\text{n-Sn}(\text{Me})_2(\text{C}_6\text{H}_3\text{-2,6-Trip}_2)$  compound. Measurement of the room-temperature spin-spin relaxation time  $T_2$  using the Carr-

Purcell technique gives  $T_2 = 3.8$  ms for the Sn(III) site at  $\delta_{\text{liq}} = +257.4$  ppm and  $T_2 = 38$   $\mu\text{s}$  for the Sn(I) site at  $\delta_{\text{liq}} = +2856.9$  ppm. An estimate of the size of the chemical shift anisotropy for the Sn(I) site can be made by assuming that  $T_2$  is governed by this anisotropy, a reasonable assumption for large, heavy molecules far from the extreme narrowing limit.<sup>18</sup> This relaxation rate in terms of the  $^{119}\text{Sn}$  gyromagnetic ratio  $\gamma$ , magnetic field  $B_0$ , correlation time  $\tau_c$ , shift tensor elements  $\delta_{\text{nn}}$ , and the isotropic shift  $\delta_{\text{iso}}$  is given by

$$\frac{1}{T_2} = \frac{2\gamma^2 B_0^2 \tau_c}{15} ((\delta_{11} - \delta_{\text{iso}})^2 + (\delta_{22} - \delta_{\text{iso}})^2 + (\delta_{33} - \delta_{\text{iso}})^2) \times 10^{-12} \quad (1)$$

where the  $10^{-12}$  is a conversion factor between ppm and absolute shielding. Taking  $\delta_{\text{iso}} \approx \delta_{\text{liq}}$  from Table 1,  $T_2 = 3.8$  ms, and the  $\delta_{\text{nn}}$  values from Table 2 for the Sn(III) site gives  $\tau_c = 261$  ns from eq 1. Using this  $\tau_c$  value along with  $T_2 = 38$   $\mu\text{s}$  and  $\delta_{\text{liq}} = +2856.9$  ppm for the Sn(II) site, the approximation of an axially symmetric shift tensor  $\delta_{22} = \delta_{33}$ , and the definition of  $\delta_{\text{iso}} = (\delta_{11} + \delta_{22} + \delta_{33})/3$  allows calculation of  $\delta_{11}$  and  $\delta_{33}$  from eq 1 as  $+7589$  ppm and  $+491$  ppm, respectively. Although an axially symmetric tensor was assumed, these values are most likely accurate to within  $\pm 1000$  ppm. Comparison of the anisotropy for these estimated components  $\chi = 7098$  ppm with  $\chi = 3798$  ppm for the X =  $\text{C}(\text{CH}_3)_3$  compound, the widest powder pattern observed in this study, indicates that the Sn(I) pattern will be about two times wider or about 1.0 MHz, well beyond both the excitation bandwidth and detection limits of the pulsed NMR spectrometer. These limitations were seen by investigating the Sn(I) site in this compound using  $^1\text{H}$ - $^{119}\text{Sn}$  cross polarization with the  $^{119}\text{Sn}$  rf carrier set to the isotropic  $+2856.9$  ppm shift. The resulting spectrum was a 50 kHz wide Gaussian line, a width directly corresponding to the rf-excitation bandwidth of the NMR spectrometer. This result supports the existence of an extremely broad chemical shift powder pattern for the Sn(I) site in the  $2,6\text{-Trip}_2\text{H}_3\text{C}_6\ddot{\text{S}}\text{n-Sn}(\text{Me})_2\text{C}_6\text{H}_3\text{-2,6-Trip}_2$  compound.

## Conclusion

The  $\delta_{\text{nn}}$  components of the shift tensor in the series of compounds with X = Cl,  $\text{Cr}(\eta^5\text{-C}_5\text{H}_5)(\text{CO})_3$ , and t-Bu can be explained on the basis of chemical structure rather than electronegativity values of the substituents. It is this point which underscores the strength of solid-state NMR over liquid-state experiments where trends in chemical shift display no apparent correlation with structural data.

**Acknowledgment.** We are grateful to the NSF for financial support. M.P.A. thanks The Packard Foundation for support.

IC000514Z

(18) Poole, C. P.; Farach, H. A. *Relaxation in Magnetic Resonance*; Academic Press: New York, 1971; p 75.